Volume 2
Number 2
April 2021
Pages 277–674

RSC Chemical Biology

rsc.li/rsc-chembio

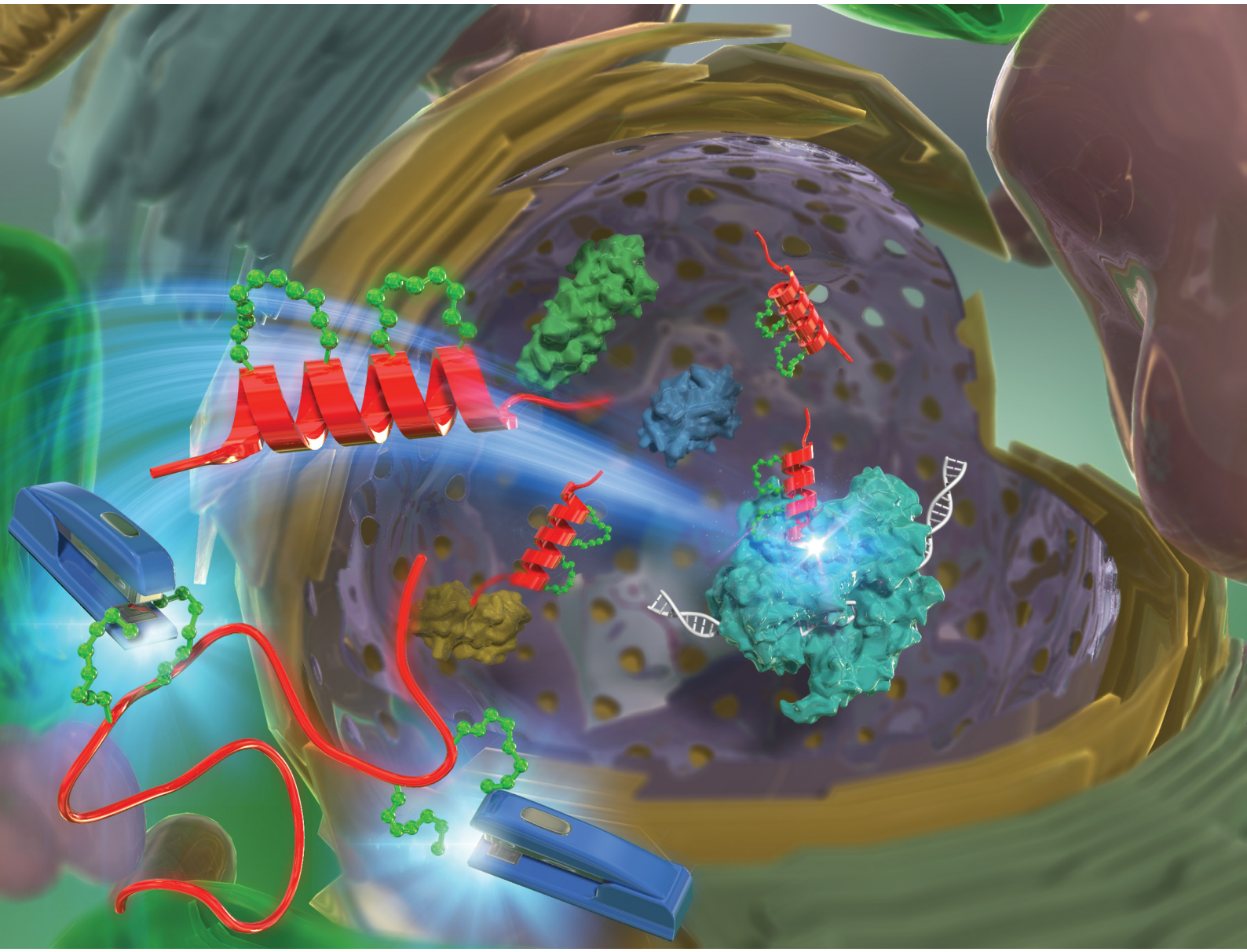

ISSN 2633-0679

ROYAL SOCIETY OF CHEMISTRY

COMMUNICATION
Yousuke Takaoka, Minoru Ueda *et al.*
Rational design of a stapled JAZ9 peptide inhibiting protein–protein interaction of a plant transcription factor

RSC Chemical Biology

ROYAL SOCIETY OF CHEMISTRY

COMMUNICATION

View Article Online
View Journal | View Issue

Check for updates

Cite this: *RSC Chem. Biol.*, 2021, 2, 499

Received 12th November 2020,
Accepted 14th December 2020

DOI: 10.1039/d0cb00204f

rsc.li/rsc-chembio

Rational design of a stapled JAZ9 peptide inhibiting protein–protein interaction of a plant transcription factor†

Kaho Suzuki,[a] Yousuke Takaoka *[a] and Minoru Ueda *[ab]

We herein describe the development of a stapled peptide inhibitor for a jasmonate-related transcription factor. The designed peptide selectively inhibited MYCs, master-regulators of jasmonate signaling, and selectively suppressed MYC-mediated gene expression in *Arabidopsis thaliana*. It is proposed as a novel chemical tool for the analysis of MYC related jasmoante signaling.

Plants are sessile and subjected to environmental changes, and have evolved unique signaling systems which include a myriad of transcription factors (TFs) under the control of small molecular plant hormones.[1,2] One of these plant hormones, jasmonoyl-L-isoleucine (JA-Ile), contributes to the regulation of plant defense responses to environmental stresses.[3,4] For example, JA-Ile causes protein–protein interactions (PPI) between F-box protein CORONATINE INSENSITIVE 1 (COI1) and jasmonate-ZIM-domain (JAZ) repressor protein,[5–7] which triggers ubiquitination and subsequent degradation of the JAZ repressors through the 26S-proteasome pathway. In the absence of JA-Ile, JAZ repressor binds to and represses various JA-related transcriptional factors including MYC, the master regulator of JA-signaling.[8,9] A variety of TFs are involved in this signaling process and responsible for a number of JA responses, including a defense response to pathogen and herbivore attack, secondary metabolite production, fertility, senescence, and growth inhibition.[8,9] Therefore, to elucidate the function of each TF, chemical tools (agonists or antagonists) specific to each individual TF are needed.[10–12]

Herein, we focus on the JAZ repressor proteins which function as hubs in this complex signaling machinery. JAZ has dual functions as a component of COI1–JAZ co-receptor and repressor of many TFs. We developed TMR-JAZ9st3, a novel stapled peptide-based MYC inhibitor, the structure of which is based on the crystal structure of JAZ9 in complex with MYC3. TMR-JAZ9st3 selectively and strongly binds MYCs, but has almost no affinity with COI1 either *in vitro* or *in planta*, and therefore could serve as a competitive inhibitor of MYC-related JA-signaling *in planta*, little affecting MYC-independent JA-signaling. Thus, TMR-JAZ9st3 would be a powerful chemical tool for the MYC-related JA-signaling pathway.

The dual function of JAZ (as a component of the COI1–JAZ co-receptor and repressor of TFs) can be explained by reference to its structure – JAZ proteins incorporate in the C-terminal region the highly conserved Jas motif, which is an established binding domain for both COI1 and MYCs.[9,13] In the reported 3D structures of the complexes of MYC3–Jas^{JAZ9} and COI1–JA-Ile–Jas^{JAZ1}, the Jas motif had undergone a dynamic structural change: the Jas^{JAZ9} peptide in complex with MYC3 forms an extended α-helix conformation, whereas the Jas^{JAZ1} peptide in complex with COI1–JA-Ile formed a bipartite conformation (N-terminal loop and C-terminal extended α-helix) (Fig. 1a). Based on these findings, a covalently 'stapled' α-helical Jas peptide would be expected to function as a MYC-selective ligand, unable to effectively bind with COI1–JA-Ile. To test this hypothesis, we designed several types of helix-stapled Jas^{JAZ9} peptides based on conventional hydrocarbon peptide stapling technology[14,15] and guided by the reported crystal structure of MYC3-Jas^{JAZ9}. Initially, four amino acids (Q221, A225, A228 and E232) in Jas^{JAZ9} were chosen as stapling sites based on their location not being in direct contact with MYC3 (Fig. 1b). Several groups recently reported bicyclic double-stapled peptides which demonstrated marked target affinity, efficient cellular uptake, and higher stability compared to the single-stapled peptides in mammalian cells.[16,17] Therefore, we designed non-stapled peptide (JAZ9wt (**1**)), two single-stapled JAZ peptides (JAZ9st1 (**2**) and JAZ9st2 (**3**)), and a double-stapled JAZ9 peptide (JAZ9st3 (**4**)), as shown in Fig. 1c. All four were covalently conjugated with the reporter tetramethylrhodamine (TMR) and evaluated for their binding affinity with MYC3. Stapled and non-stapled peptides were synthesized using SPPS and purified by HPLC and characterized by MALDI-TOF MS analyses after cleavage from the resin (Scheme S1 and Fig. S1 and S2, ESI†).

[a] *Graduate School of Science, Tohoku University, 6-3, Aramaki-Aza-Aoba, Aoba-ku, Sendai, 980-8578, Japan. E-mail: ytakaoka@tohoku.ac.jp*
[b] *Graduate School of Life Science, Tohoku University, 6-3, Aramaki-Aza-Aoba, Aoba-ku, Sendai, 980-8578, Japan*

† Electronic supplementary information (ESI) available. See DOI: 10.1039/d0cb00204f

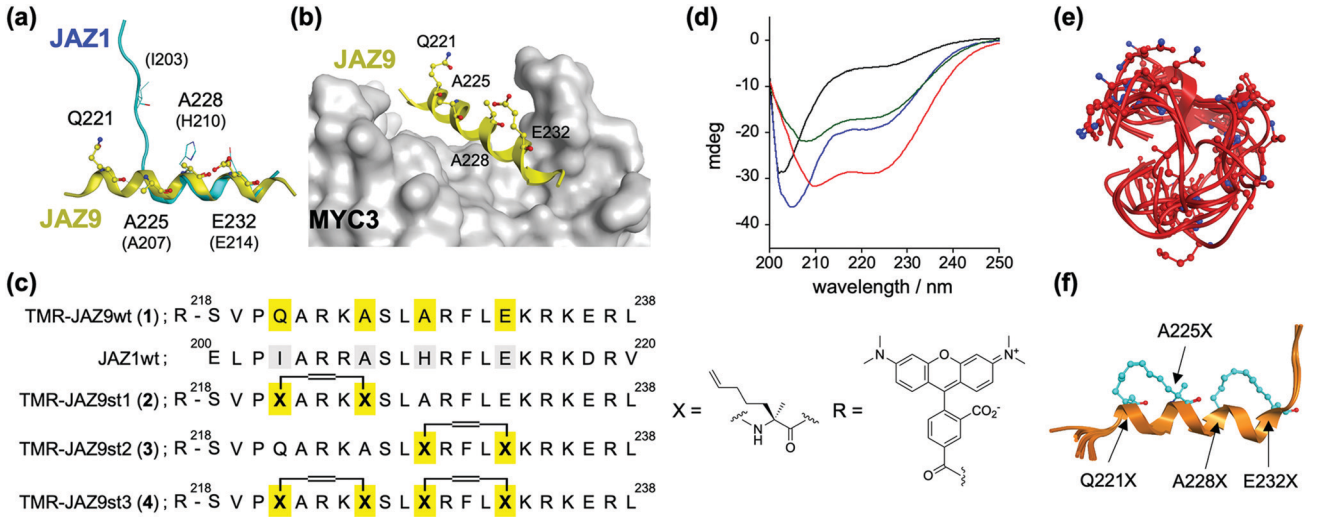

Fig. 1 (a) Superimposed structures of Jas^{JAZ1} (cyan) complexed with COI1–JA-Ile (PDB ID: 3OGL) or Jas^{JAZ9} (yellow) complexed with MYC3 (PDB ID: 4RS9). (b) Crystal structure of MYC3–JAZ9 showing the stapling sites (PDB ID: 4RS9). (c) Molecular design of stapled JAZ9-peptides with amino acid sequences of Jas^{JAZ1}/Jas^{JAZ9}, and chemical structures of the building block for stapling (X) and tetramethylrhodamine (R). (d) CD spectra of TMR-JAZ9 peptides (each 10 μM) (**1**; black, **2**; blue, **3**; green, **4**; red) in PBS buffer (pH 7.4). (e and f) Superposition of the most stable top 5 model structures obtained by conformational searching with MD simulation; (e) JAZ9wt, (f) JAZ9st3. The amino acids at the stapling sites (Q221X, A225X, A228X, and E232X) are shown as stick models.

The helicities of the synthesized stapled peptides were examined by circular dichroism (CD) experiments. From these results (Fig. 1d), **1** was inferred to form a random loop structure in the buffer solution (the helix content was calculated to be 6%, and random structure to be 81%, respectively).[18] The 3D structure of this peptide was predicted to be mainly disordered and random, by conformational searching with an MD simulation (Fig. 1e). In contrast, the ellipticity values of the stapled peptides at both 208 nm and 220 nm grow negatively, and the helix contents of these peptides were calculated to be 25, 25, and 45%, for **2**, **3**, and **4**, respectively (Fig. 1d). The predicted 3D structures by the *in silico* MD simulation also supported these results (Fig. 1e, f and Fig. S3, ESI†). The helicities of the top five predicted structures of these peptides were calculated to be 8%, 31%, 32%, or 68% for JAZ9wt, JAZ9st1, JAZ9st2, or JAZ9st3, respectively, consistent with the analyses by CD. These results demonstrated that the 3D structure of Jas^{JAZ9} peptide is intrinsically disordered, and the helicities of our stapled peptides increased with increasing stapling number.

To examine the affinity of these stapled peptides for MYCs and COI1–JA-Ile, we prepared the JAZ-binding domains of MYC and COI1 (His6-SUMO-tagged MYC2(55-259), MYC3(44-238), MYC4(55-253), and GST-tagged COI1(full-length)) according to the previous reports.[7,10,19] The interaction between MYC3 and non-stapled or stapled peptides (**1**–**4**) was confirmed using the AlphaScreen inhibitory assays between His6-SUMO-MYC3 and biotin-conjugated Jas^{JAZ9}.[19] As shown in Fig. 2a, all four peptides competitively inhibited the MYC-Jas^{JAZ9} interaction; the IC50 value of **4** was determined to be 2.7 μM, 10-fold lower than that of **1**, and clearly demonstrating that our stapled peptides are more potent inhibitors of MYC3 compared with non-stapled JAZ9 peptide (Table 1).

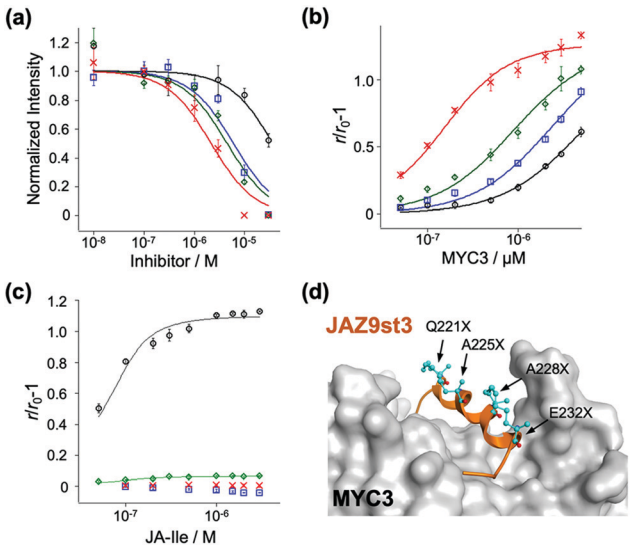

Fig. 2 (a) Inhibition curves of TMR-JAZ9 peptides for His6-SUMO-MYC3 and biotin-JAZ9 peptide by AlphaScreen assay (**1**; black circle, **2**; blue square, **3**; green diamond, **4**; red cross). Experiments were performed in triplicate to obtain mean and S.D. (shown as error bars). (b) FA change of TMR-JAZ9 peptides upon addition of MYC3 (0–5 μM). Experiments were performed in triplicate to obtain mean and S.D. (shown as error bars). (c) FA change of TMR-JAZ9 peptides and GST-COI1 upon addition of JA-Ile (0–3 μM). Experiments were performed in triplicate to obtain mean and S.D. (shown as error bars). (d) The model structure obtained by docking simulation of JAZ9st3 (orange ribbon, the amino acids at the stapling sites (Q221X, A225X, A228X, and E232X) were shown as cyan ball-and-stick models) and MYC3 (gray).

Quantitative evaluation of the binding affinity was accomplished in a fluorescence anisotropy (FA) assay; the FA values of these

Table 1 The affinity values of TMR-JAZ9 peptides with MYCs or COI1/JA-Ile

	MYC3		MYC2	MYC4	COI1–JA-Ile
	IC50[a]/μM	K_d[b]/μM	K_d[b]/μM	K_d[b]/μM	K_d[b]/nM
TMR-JAZ9wt (**1**)	37 ± 10	5.0 ± 1.1	3.6 ± 0.8	11 ± 3.7	15 ± 4.3
TMR-JAZ9st1 (**2**)	6.0 ± 1.6	2.4 ± 0.5	1.5 ± 0.2	2.6 ± 0.3	n.d.[c]
TMR-JAZ9st2 (**3**)	4.5 ± 1.4	0.88 ± 0.2	0.73 ± 0.1	1.5 ± 0.2	29 ± 11
TMR-JAZ9st3 (**4**)	2.2 ± 0.5	0.10 ± 0.02	0.16 ± 0.06	0.88 ± 0.2	n.d.[c]

[a] The values were obtained by AlphaScreen, shown in Fig. 2a. [b] The values were obtained by FA experiments, shown in Fig. 2b, c and Fig. S4 (ESI). [c] The value could not be determined due to the low signal change.

peptides were significantly increased upon addition of His6-SUMO-MYC3 in a dose dependent manner (Fig. 2b). The apparent K_d value of **1** with His6-SUMO-MYC3 was calculated to be 5.0 μM (Table 1). In contrast, the K_d value of **4** was 0.10 μM, which is 50-fold, 24-fold, or 8.8-fold lower than that of **1**, **2** or **3**, respectively (Table 1). The significant enhancement in the affinity of the double-stapled peptide was also observed in the cases of MYC3 isoforms, MYC2 and MYC4 (Fig. S4, ESI† and Table 1). Moreover, the stapled peptide **4** showed similar affinity to all MYC isoforms (0.10, 0.16, or 0.88 μM for MYC3, MYC2, or MYC4, respectively), which is consistent with the sequence homology analysis of the binding sites of these three MYCs for a JAZ (Fig. S5, ESI†). These results suggest that the secondary structure of the Jas motif comprises an extended helix when interacting with MYC2 or MYC4, as is the case with MYC3.

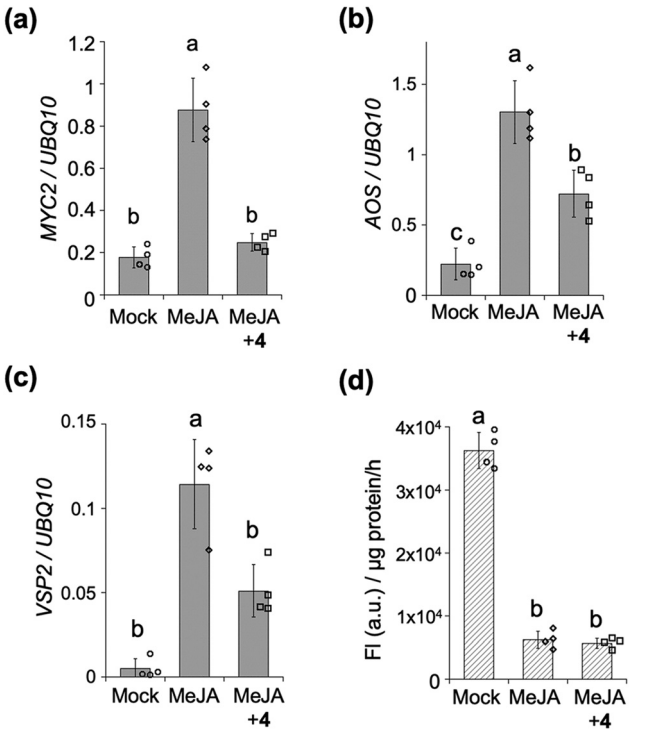

Fig. 3 (a–c) Analysis of the expression of JA-responsive marker genes (a; *MYC2*, b; *AOS*, c; *VSP2*) by quantitative RT-PCR in 7-d-old Arabidopsis seedlings (Col0) with or without chemicals (MeJA, or MeJA and **4**, 10 μM respectively) (n = 4). The seedlings were treated with chemicals for 2 h (*MYC2*, *AOS*) or for 8 h (*VSP2*). (d) Quantification of GUS activity in five roots of 4-d-old 35S:JAZ1-GUS plants (n = 4). Seedlings were pretreated for 1 h with or without chemicals (MeJA, or MeJA and **4**, 10 μM respectively). Experiments were repeated at least three times with similar results, and significant differences were evaluated by one-way ANOVA/Tukey HSD *post hoc* test ($p < 0.01$).

To verify the target selectivity of our stapled peptides, we undertook a binding assay with COI1–JA-Ile, by FA-based methods.[20] Upon addition of JA-Ile to a solution of GST-COI1 and **1**, the FA values were significantly increased (Fig. 2c). The apparent K_d value with **1** and GST-COI1 was 13 nM, consistent with previous results (Table 1) (K_d was found to be 10 nM, by using fluorescein-conjugated JAZ9wt).[20] A similar value was obtained with **3**, a single stapled peptide in the C-terminal region of the Jas motif which will have the same N-terminal random loop conformation when it binds with COI1 (Fig. 2c and Table 1). In contrast, no significant change in FA value was observed for **2** and **4**, which are stapled in the N-terminal region of the Jas motif (Fig. 2c). These results clearly demonstrate that the double-stapling strategy markedly enhances the binding affinity for MYCs and selectivity for MYCs over COI1.

To better understand the binding between the designed peptides with MYC3, we undertook an *in silico* molecular docking simulation. As shown in Fig. 2d and Fig. S6 (ESI†), the double stapled JAZ9 peptide (JAZ9st3) was found to tightly bind to MYC3, without perturbation of this interaction by the stapling sites of JAZ9st3. These results suggest that our design strategy was largely successful both thermodynamically and structurally.

We next assessed the inhibitory effect of the stapled peptide **4** on MYC-mediated gene expression in Arabidopsis seedlings – treatment of which with methyl jasmonate (MeJA, a precursor of JA-Ile) was previously reported to strongly upregulate the expression of MYC-regulated marker genes such as *MYC2*, *JAZ1*, *LOX2*, *AOS* (JA-Ile biosynthesis) or *VSP2* (defense responses) (Fig. 3a–c and Fig. S7, ESI†).[21,22] Upon co-treatment of the seedlings with MeJA and **4**, the expression of these MYC-mediated marker genes was significantly suppressed (Fig. 3a–c and Fig. S7, ESI†). The extent of inhibition of the expression of *AOS* and *VSP2* was found to depend on the dose of **4**, up to 20 μM (Fig. S8, ESI†), whereas the expression of *AOS* was upregulated in the presence of 50 μM of **4** (data not shown). Very little inhibition of the expression of *AOS* or *VSP2* was observed with **1** (Fig. S9, ESI†), indicating that the inhibition of MeJA-mediated expressions of MYC-regulated genes *in vivo* by stapled **4** can be attributed to its much higher binding affinity for the MYCs compared to the non-stapled **1**.

The MYC-selective affinity of the double-stapled peptide **4** suggested it to have a COI1-independent function *in planta*.

COI1-dependent signaling *in planta* can be quantified using transgenic β-glucuronidase (GUS)-reporter line (*35S: JAZ1-GUS*): MeJA causes degradation of the JAZ1-GUS fusion protein through COI1, and the downstream signaling could be quantified as reduced GUS staining (Fig. 3d and Fig. S10, ESI†). This degradation was also observed even in the presence of **4**, demonstrating that **4** does not affect the interaction between COI1 and JAZ *in vivo* as well as *in vitro*.

Conclusions

In conclusion, a double-stapled JAZ9 peptide selective inhibitor of MYC TFs, the master regulator of jasmonate signaling, has been designed based on the crystal structure of MYC3–Jas^{JAZ9}, and tested.[19] The 3D structure of this peptide resembles a helix structure as MYC3-binding form, resulting in a 50-fold higher affinity for MYC3 compared to the non-stapled peptide – perhaps due to chemical stabilization of the 3D structure of the peptide entropically favoring binding with MYC3. Such affinity enhancement was also observed for MYC2 and 4, suggesting that the MYC family proteins bind to the Jas motif in a manner similar to that for MYC3; analysis of the 3D structures of MYC2 and 4 is pending. In contrast, no binding was observed between our double-stapling peptide and COI1–JA-Ile – presumably because this peptide cannot form a loop structure as COI1-binding form.[7] Moreover, our double-stapled peptide **4** could suppress the jasmonate-induced MYC-related gene expression in *Arabidopsis thaliana*, demonstrating that our peptide would be a useful chemical tool for analyses of the MYC-related jasmonate signaling, as well as open the door to develop various peptide-based functional ligands *in planta* in the future.

Conflicts of interest

The authors declare no competing financial interest.

Acknowledgements

We thank Prof. S. Nishizawa and Dr. Y. Sato (Tohoku University) for the use of the circular dichroism spectrometer. We also thank Mr. D. Kanayama (Tohoku University) for his technical support on AlphaScreen assay, and Ms. Ika N. Azizah (Tohoku University) for her technical support on protein preparation and peptide synthesis. This work was financially supported by a Grant-in-Aid for Scientific Research from JSPS, Japan (no. 17H06407, 18KK0162, and 20H00402 for MU, and 19H05283 for YT), JSPS A3 Foresight Program (MU), JSPS Core-to-Core Program Asian Chemical Biology Initiative (MU), JST-PREST Grant JPMJPR16Q4 (YT), and Takeda Science Foundation (YT).

Notes and references

1 A. Santner and M. Estelle, *Nature*, 2009, **459**, 1071–1078.
2 T. A. Meraj, J. Fu, M. A. Raza, C. Zhu, Q. Shen, D. Xu and Q. Wang, *Genes*, 2020, **11**, 346.
3 C. Wasternack and B. Hause, *Ann. Bot.*, 2013, **111**, 1021–1058.
4 S. Fonseca, A. Chini, M. Hamberg, B. Adie, A. Porzel, R. Kramell, O. Miersch, C. Wasternack and R. Solano, *Nat. Chem. Biol.*, 2009, **5**, 344–350.
5 A. Chini, S. Fonseca, G. Fernandez, B. Adie, J. M. Chico, O. Lorenzo, G. Garcia-Casado, I. Lopez-Vidriero, F. M. Lozano, M. R. Ponce, J. L. Micol and R. Solano, *Nature*, 2007, **448**, 666–671.
6 B. Thines, L. Katsir, M. Melotto, Y. Niu, M. Ajin, G. Liu, K. Nomura, S. Y. He, G. A. Howe and J. Browse, *Nature*, 2007, **448**, 661–665.
7 L. B. Sheard, X. Tan, H. Mao, J. Withers, G. Ben-Nissan, T. R. Hinds, Y. Kobayashi, F. F. Hsu, M. Sharon, J. Browse, S. Y. He, J. Rizo, G. A. Howe and N. Zheng, *Nature*, 2010, **468**, 400–405.
8 L. Pauwels and A. Goossens, *Plant Cell*, 2011, **23**, 3089–3100.
9 A. Chini, S. Gimenez-Ibanez, A. Goossens and R. Solano, *Curr. Opin. Plant Biol.*, 2016, **33**, 147–156.
10 Y. Takaoka, M. Iwahashi, A. Chini, H. Saito, Y. Ishimaru, S. Egoshi, N. Kato, M. Tanaka, K. Bashir, M. Seki, R. Solano and M. Ueda, *Nat. Commun.*, 2018, **9**, 3654.
11 C. Meesters, T. Monig, J. Oeljeklaus, D. Krahn, C. S. Westfall, B. Hause, J. M. Jez, M. Kaiser and E. Kombrink, *Nat. Chem. Biol.*, 2014, **10**, 830–836.
12 I. Monte, M. Hamberg, A. Chini, S. Gimenez-Ibanez, G. Garcia-Casado, A. Porzel, F. Pazos, M. Boter and R. Solano, *Nat. Chem. Biol.*, 2014, **10**, 671–676.
13 A. Wager and J. Browse, *Front. Plant Sci.*, 2012, **3**, 41.
14 C. E. Schafmeister, J. Po and G. L. Verdine, *J. Am. Chem. Soc.*, 2000, **122**, 5891–5892.
15 P. M. Cromm, J. Spiegel and T. N. Grossmann, *ACS Chem. Biol.*, 2015, **10**, 1362–1375.
16 G. H. Bird, N. Madani, A. F. Perry, A. M. Princiotto, J. G. Supko, X. He, E. Gavathiotis, J. G. Sodroski and L. D. Walensky, *Proc. Natl. Acad. Sci. U. S. A.*, 2010, **107**, 14093–14098.
17 G. J. Hilinski, Y.-W. Kim, J. Hong, P. S. Kutchukian, C. M. Crenshaw, S. S. Berkovitch, A. Chang, S. Ham and G. L. Verdine, *J. Am. Chem. Soc.*, 2014, **136**, 12314–12322.
18 A. Micsonai, F. Wien, L. Kernya, Y.-H. Lee, Y. Goto, M. Réfrégiers and J. Kardos, *Proc. Natl. Acad. Sci. U. S. A.*, 2015, **112**, E3095–E3103.
19 F. Zhang, J. Yao, J. Ke, L. Zhang, V. Q. Lam, X. F. Xin, X. E. Zhou, J. Chen, J. Brunzelle, P. R. Griffin, M. Zhou, H. E. Xu, K. Melcher and S. Y. He, *Nature*, 2015, **525**, 269–273.
20 Y. Takaoka, K. Nagumo, I. N. Azizah, S. Oura, M. Iwahashi, N. Kato and M. Ueda, *J. Biol. Chem.*, 2019, **294**, 5074–5081.
21 O. Lorenzo, J. M. Chico, J. J. Sanchez-Serrano and R. Solano, *Plant Cell*, 2004, **16**, 1938–1950.
22 F. Schweizer, P. Fernandez-Calvo, M. Zander, M. Diez-Diaz, S. Fonseca, G. Glauser, M. G. Lewsey, J. R. Ecker, R. Solano and P. Reymond, *Plant Cell*, 2013, **25**, 3117–3132.